Ab initio periodic Hartree-Fock study of lizardite 1*T*

ĽUBOMÍR SMRČOK AND ĽUBOMÍR BENCO

Institute of Inorganic Chemistry, Slovak Academy of Sciences, SK-842 36 Bratislava, Slovak Republic

ABSTRACT

A periodic ab initio Hartree-Fock LCAO study was performed on the 1:1 sheet silicate lizardite, $Mg_3Si_2O_5(OH)_4$, which has $P31m$ symmetry. A total of 258 atomic orbitals were described using double-zeta-quality basis sets augmented with polarization d (Si, Mg, O) and p (H) functions. Density of states and electron charge-density maps were calculated to investigate the electronic properties. The majority of the valence states are composed of O and Si atomic orbitals with little contribution from H atoms. Calculations showed that although there are about 0.5|e| in Si d and about 0.1|e| in Mg d orbitals, the population of O d orbitals is negligible. The maps of charge density show that interlayer hydrogen bonds fix adjacent 1:1 layers. Positions of the main O peaks in projected density of states evaluated for both three-dimensional (3D) and two-dimensional (2D) calculations were influenced by layer-to-layer interactions, especially hydrogen bonds.

INTRODUCTION

The trioctahedral 1:1 layer silicate lizardite, with ideal chemical composition $Mg_3Si_2O_5(OH)_4$, is interesting from the viewpoint of theoretical chemistry. The structure consists of 2D sheets held together by weak forces along the *c* axis and provides an excellent case study of three types of coexisting chemical bonds: strong covalent bonds between Si and O in the tetrahedral sheet, ionic bonds between Mg and O in the octahedral sheet, and rather weak hydrogen bonds holding the individual 1:1 layers together. However, most previous analyses of bonding in lizardite have been supported by indirect evidence such as O-H ⋯ H distances or by the expected similarity of Si-O and Mg-O bonds in lizardite to those in analogous compounds treated by quantum chemical methods, e.g., MgO (Causà et al. 1986), brucite (Sherman 1991; D'Arco et al. 1993), $MgSiO_3$ (Nada et al. 1992), or kaolinite (Hess and Saunders 1992).

The aim of this study is to characterize the presence of the three types of bonding in lizardite by theoretical ab initio calculations and to describe the electronic structure of the mineral in several important regions of the unit cell.

METHODS

All calculations were made using the self-consistent–field linear combinations of atomic orbitals (SCF LCAO) Hartree-Fock program for periodic systems, CRYSTAL (Dovesi et al. 1992). This approach is much more powerful than cluster methods or electrostatic approaches, which often provide rather doubtful results for systems with significant covalent bonds, e.g., silicates. This method accounts for translational symmetry, and hence the whole crystal field is considered (Pissani et al. 1988). Crystal orbitals are expanded in Bloch functions, which are expressed on the basis of atomic orbitals (AO). Thus, the arbitrariness introduced by the terminal atoms and the size of a cluster isolated from the solid is removed.

GEOMETRY AND COMPUTATIONAL DETAILS

The positions of all atoms in the unit cell of the 1*T* polytype of lizardite were derived from the single-crystal structure refinement of Mellini (1982). The computational cell, based on the space group $P31m$, includes three Mg, two Si, ten O, and three H atoms. It was assumed that the structure represents equilibrium, or at least an equilibrium configuration. A total of 258 AOs were described by Huzinaga's double-zeta basis functions enriched with polarization d and p functions (Huzinaga 1965). The basis sets used are as follows: O, (8s4p)/[4s2p] + 1d (1.2); Si, (11s7p)/[6s4p] + 1d (0.4); Mg, (9s5p)/[5s3p] + 1d (0.23); H, (4s)/[2s] + 1p (0.8). (The exponents of polarization functions were set at the values used in molecular studies.) The *k* space was sampled in 60 *k* points, the SCF-convergence criterion was $\sim 10^{-8}$ a.u. (atomic units, 1 a.u. $\approx 4.36 \times 10^{-18}$ J) of total energy, and the input tolerances for the calculation of the infinite Coulomb and exchange series were $s_c = t_m = s_{ex} = p_{ex}^g = 6$ and $p_{ex}^l = 12$, respectively (Pissani et al. 1988). The high symmetry of the structure significantly limits the amount of two-electron integrals to an acceptable number.

RESULTS AND DISCUSSION

Density of states (DOS)

Total DOS is partitioned into two main bands characterized by their dominant components as the s and p bands (Fig. 1), though, as shown below, neither band is made up exclusively of either s or p orbitals. The s band, spanning −37 to −33 eV, has a simpler structure than the p band, which has bonding and nonbonding regions for-
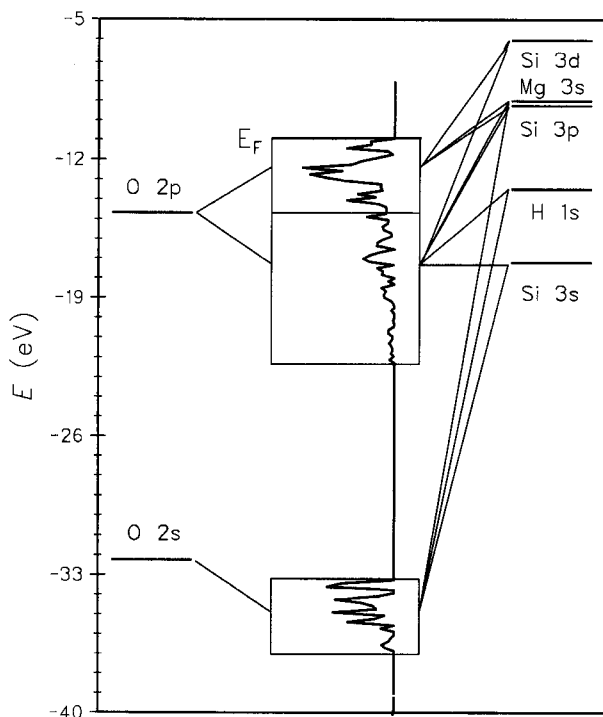
FIGURE 1. Sketch of the crystal orbital scheme of lizardite. Total DOS is vertically positioned in the center; the interaction lines connecting the most important atomic levels to the DOS bands indicate how the s band (bottom) and the p band (top) are composed. E_F indicates the position of the Fermi level.

mally separated by the O 2p atomic level at approximately -14.8 eV. The states below this level are the bonding states, i.e., they are stabilized, whereas those above the O 2p atomic level are nonbonding, i.e., destabilized.

Contributions of individual AOs to particular bands of a total DOS are easy to identify through the projected density of states (PDOS). Projections were made for the sets of s, p, and d orbitals of chemically distinct groups of atoms. Ideally, calculated PDOS can be compared with experimental X-ray emission spectra (XPS), but to our knowledge no such spectra have been published for lizardite.

The p band. Contributions of s and p orbitals of four unique groups of O atoms to the p band are shown in Figure 2a. The O groups, which differ in their chemical environments, are as follows: The basal O atom (O_B), which is the connecting O atom within the tetrahedral layer; the apical O atom (O_A), which interfaces the tetrahedral and octahedral layer; the close-packed O atoms of the outer OH groups (O_O); and, finally, the O atoms of the inner OH groups (O_I), which are raised (toward the octahedral Mg atoms) 0.064 Å from the quasi plane of O_A.

The majority of O 2p states, with the exception of O_B, are found between O 2p and Fermi level (E_F) lines, in-

dicating that they are nonbonding, e.g., lone electron pairs. These states are destabilized in comparison with the O 2p atomic level, but they help to stabilize part of the Mg 3s and Si 3p states (Fig. 1). The most stable O states in the p band originate from p orbitals of O_B plus small contributions of s orbitals from O_B and O_A.

The strong covalent nature of the Si-O_B bond is confirmed by the identical bonding states of O_B and Si bonding states (Fig. 2b). This effect is especially pronounced in the region near -19 eV. Of the three possible Si contributions (s, p, and d) to the p band, s orbitals are more stabilized in comparison with p orbitals. The d orbitals, though partially occupied (see below), participate primarily in nonbonding states.

The contribution of Mg p orbitals to the p band is negligible. The sparsely occupied Mg d orbitals are similar to the Si d orbitals (Fig. 2c).

Finally, occupied states originating from H(s) orbitals and contributing to the p band are illustrated in Figure 2d. Their positions well below E_F clearly indicate that they are involved in strong covalent bonds to corresponding O atoms of respective OH groups. All occupied H states consisting of s orbitals are strongly stabilized, having negligible contribution to nonbonding states. On the other hand, H p orbitals play a very small role in covalent O-H bonds.

The s band. Contributions of O p orbitals to the s band (Fig. 3a) are insignificant, like those of s orbitals to the p band. The positions of the main peaks of four inequivalent O types are so different that it may be suggested that they would be distinct in an XPS spectra. The structure of the O_B bands is more pronounced than that of the O_A bands, which reflects the different bonding environments. Because of their special role, the states of O_A are the least stabilized of all O states within the s band. Apical O atoms collect charge from surrounding Si and Mg atoms and are therefore involved in more polar bonds. The states of the O atoms of the inner OH groups are, relative to the situation in the p band, more stabilized than those of the outer OH groups. One possible interpretation is given below.

The contributions of Si s, p, and d orbitals to the s band are evident in Figure 3b. Again, mirror images of the O_B states and to lesser extent O_A states appear, confirming the covalent character of Si-O_B and Si-O_A bonds. The contributions of Mg atoms to the s band are small, as in the p band (Fig. 3c). In contrast, the nearly perfect coincidence of the O and H atom states of OH reveals strong covalent bonds (Fig. 3d).

Charge densities

To investigate the interactions between the atoms, both charge-density and deformation-density maps were evaluated. Charge-density maps provide information on spatial distribution of electron density and depict the interatomic interactions, whereas deformation maps show the changes in electron density that are due to chemical bonds. Both kinds of densities were sampled in three
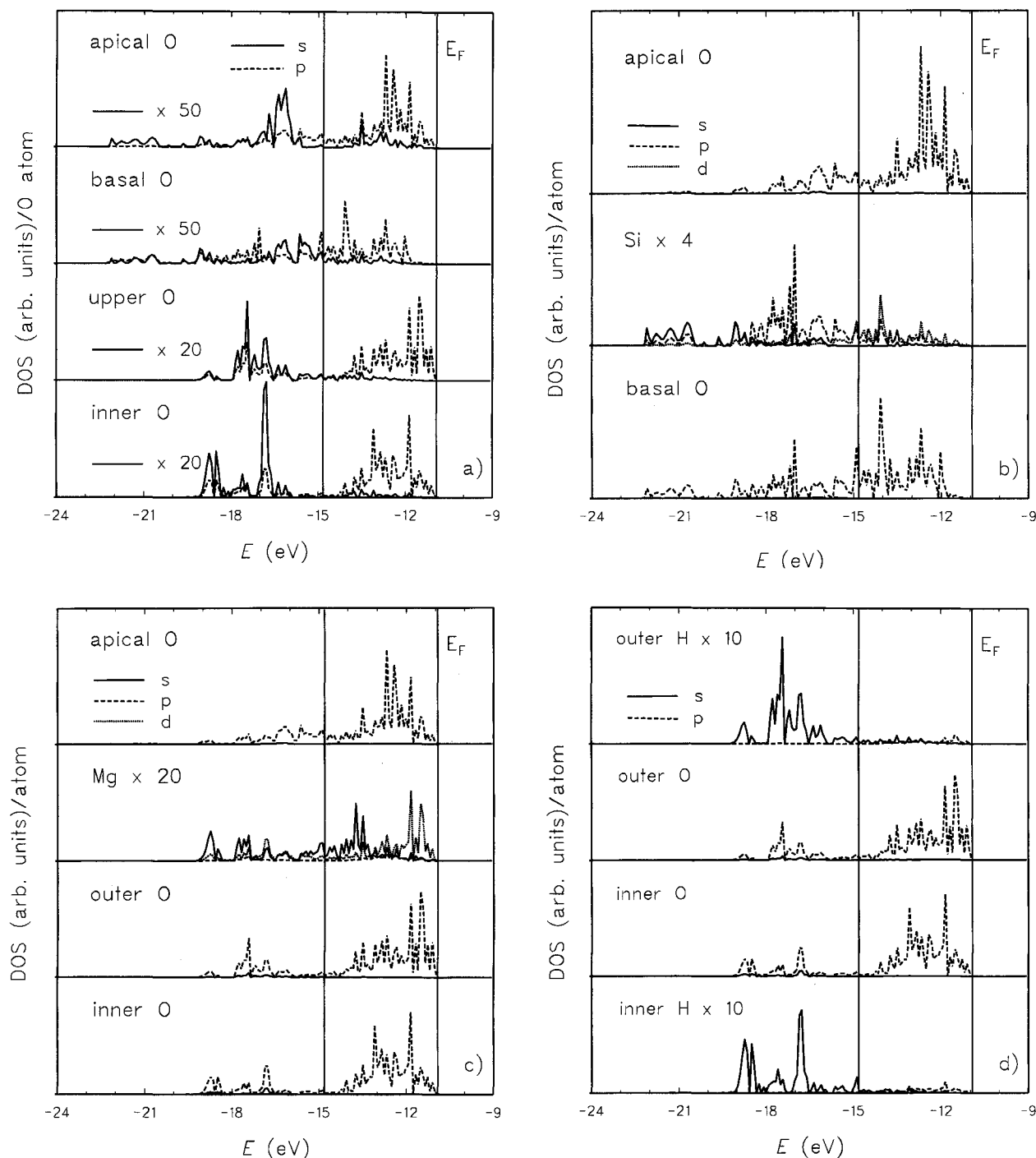
FIGURE 2. Projected DOS of the p band of lizardite. The vertical line on the left of the Fermi level (E_F) is the O 2p level.

planes, A, B, and C (Fig. 4), which cut the structure parallel to the c axis.

The A plane, bisecting the ditrigonal cavity and two O_B atoms, provides information on electron densities around the Mg atom and the inner and outer OH groups (Fig. 5a). Distribution of electron density near the Mg atom is spherical, but low isolines are slightly deformed on the contacts to neighboring OH groups. Because there is no significant overlap between electron densities around Mg and O atoms, the Mg-O bond is highly ionic. This is confirmed by the corresponding deformation map (Fig. 5b), showing a decrease of charge in the region
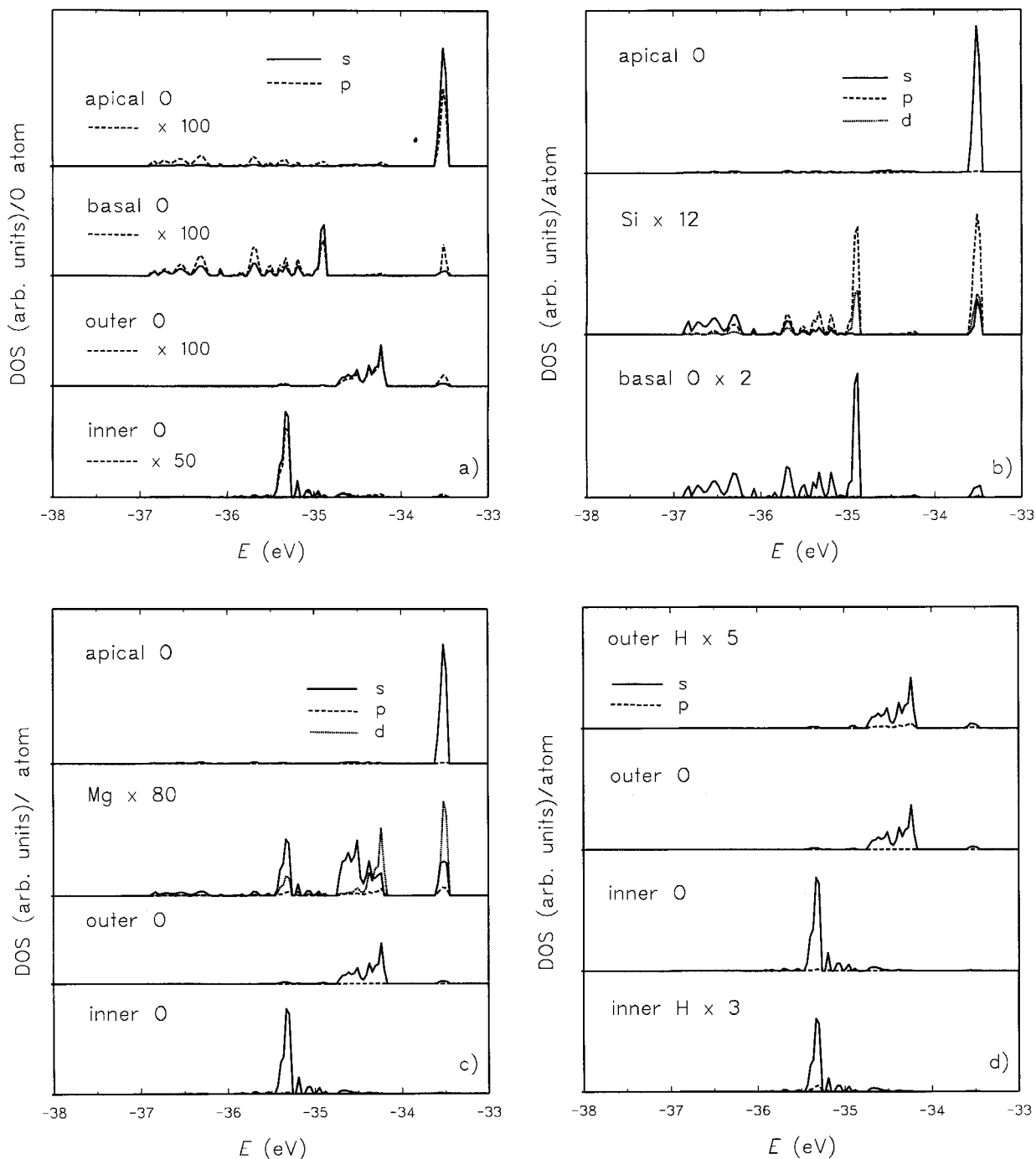
FIGURE 3. Projected DOS of the s band of lizardite.

between Mg and O. In contrast, the great overlap of electron densities for the O-H bond completely obscures the individual atoms, indicating a very covalent bond. Naturally, the formation of the covalent O-H bond corresponds to an increase of electron density in the interatomic region, as shown in Figure 5b. The formation of chemical bonds is also responsible for some contraction

of electron density near OH groups, seen as an asymmetric density cloud. The regions of depleted electron density near H atoms (Fig. 5b) are the result of electron-density transfer to the covalent bond. Each O atom of an OH group is therefore simultaneously involved in two kinds of chemical bonds: one highly ionic, the other strongly covalent. The contact between an O_B atom and
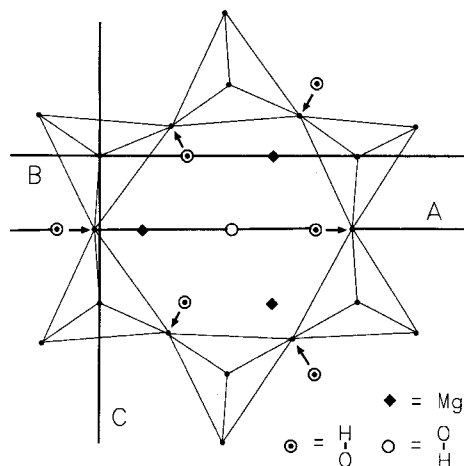
Figure 4. The top view of a six-membered ring of SiO$_4$ tetrahedra with projection planes A, B, and C.

toward the Si atom but spherical toward the Mg atom. The contact Mg-O$_O$ does not differ from Mg-O$_A$, which indicates the highly isotropic character of electron density around Mg atoms.

A decrease of electron density around Si and Mg is in both cases significant but different (Fig. 6b): Around the Si atom the density has a strongly anisotropic character, reflecting polar covalent bonds, whereas around Mg it is distributed almost evenly with a shallow minimum.

The C cross section shown in Figure 7 illustrates the strong overlap of electron densities in covalent bonds of the tetrahedral layer. The electron density near O$_A$ is slightly elongated, whereas the distribution near O$_B$ is distorted in two directions. Electron density is deformed along the Si-O$_B$-Si bridge, indicating strong covalent bonds forming the six-membered silicate rings. More details concerning the bonds in the tetrahedral sheet are discussed in Benco and Smrčok (1994).

Mulliken population analysis

An overview of electron transfer in lizardite is given by the results of a conventional Mulliken population analysis (Tables 1 and 2). The important role of Si d and to lesser extent Mg d orbitals is documented by their electron populations. In contrast, nearly zero populations of O d orbitals confirm their small role in bond formation. Enrichment of the H basis set with polarization p orbitals resulted not only in a significant drop of the total energy of ~0.03 a.u./unit cell in comparison with a preliminary calculation done without H p, but in a remarkable alteration of charges of all H atoms as well. Questionable charges dropped from approximately +0.34|e| to the val-
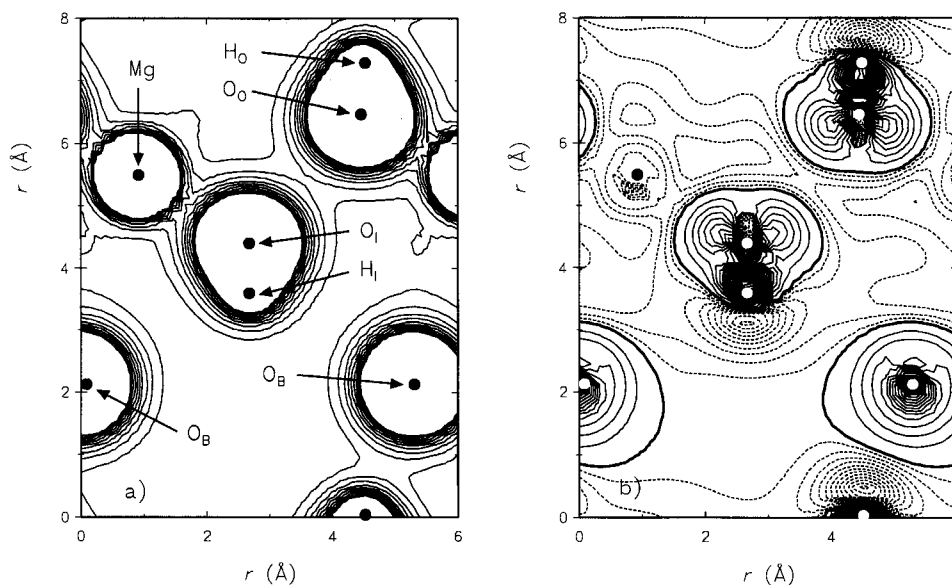
an H atom (Figs. 5a and 5b) belonging to the adjacent 1:1 layer results in increase of electron density (see below). Interestingly, there is no apparent interaction between the H atom of the inner OH group and the O$_B$ atom.

Figure 5 provides insight into the bonding within the octahedral layer, and Figure 6 illustrates bonding between 1:1 layers (cross-section B). Differences between ionic Mg-O,OH and covalent Si-O bonds are evident, as is the role of interfacing (apical) O atoms. Note that the overlap of electron densities in Si-O bonds is not as pronounced as in the O-H bond.

The electron density around interfacing O$_A$ is elongated

Figure 5. (a) Contour map of total charge density sampled in plane A (cf. Fig. 4). Solid circles indicate atom positions. Cutoff is at 0.1 e/bohr^3; contour-line spacing is 0.01 e/bohr^3. (b) Density-deformation map in plane A. Thin, thick, and dashed lines indicate positive, zero, and negative values, respectively. Contour-line spacings are 0.008 e/bohr^3 for positive values and 0.0025 e/bohr^3 for negative values.

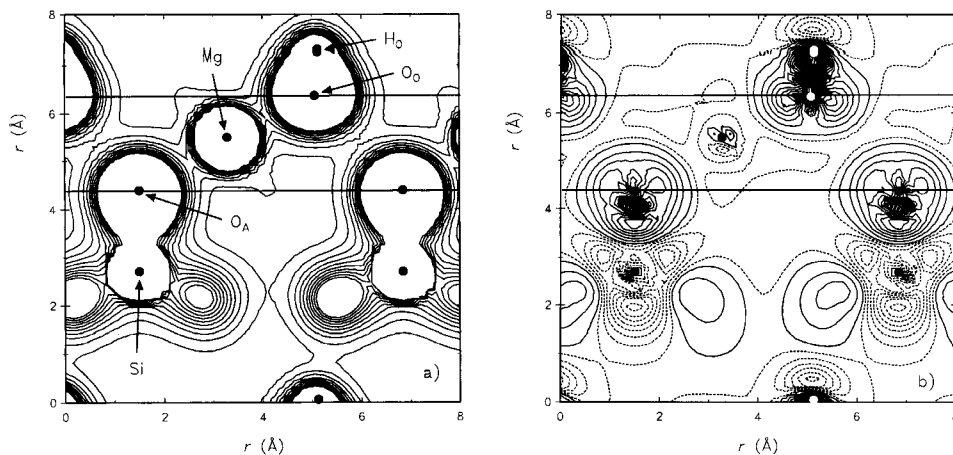**Figure 6.** (a) Contour map of total charge density sampled in plane B (cf. Fig. 4). Cutoff is at 0.1 e/bohr³; contour-line spacing is 0.01 e/bohr³. (b) Density-deformation map in plane B. Contour-line spacings are 0.008 e/bohr³ for positive values and 0.004 e/bohr³ for negative values.

ues in Table 1. Consequently, those changes also induced noticeable changes in the charges of O atoms, which became on average ~0.23|e| more negative.

The most important bond populations and the corresponding interatomic distances are given in Table 2. Large positive bond populations indicate strong covalent bonds, negative values indicate antibonding (repulsion), and zero values indicate nonbonding. All positive values in Table 2 support the evidence given above: The small negative values for O-O repulsions indicate that they do not play a fundamental role. The O ··· H bond population (+5 to +10) is small. These values may be compared to +4 for brucite (D'Arco et al. 1993) and +30 and +40 for hydrogen bonds in bulk urea (Dovesi et al. 1990).

Interactions in the c direction

Adjacent 1:1 layers are held together by two principal forces: nondirectional dispersive (presumably weak) layer-to-layer interactions and directional hydrogen bonds. The former interactions are rather difficult to model. An attempt to quantify them would require comparison of two polytypes with different stacking sequences, e.g., the $2H_1$ polytype (Mellini and Zanazzi 1987) and a hypothetical $2T$ polytype. Unfortunately, such calculations with a basis set of double-zeta quality similar to that of the basis set used in this study were beyond the capabilities of our facilities.

On the other hand, the hydrogen bonds were easier to investigate. Their binding role in lizardite was examined
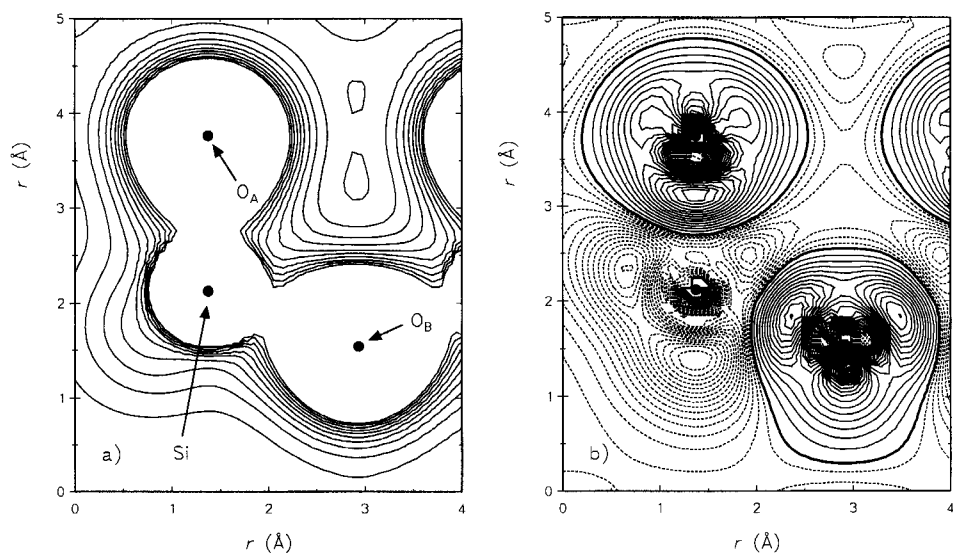

Figure 7. (a) Contour map of total charge density sampled in plane C (cf. Fig. 4). Cutoff is at 0.1 e/bohr³; contour-line spacing is 0.01 e/bohr³. (b) Density-deformation map in plane C. Contour-line spacings are 0.004 e/bohr³ for positive values and 0.002 e/bohr³ for negative values.

TABLE 1. Mulliken charges and bond populations (in $10^{-3}|e|$ units) of polarization orbitals

| Atom	3D			2D		
	Charge	d	p	Charge	d	p
Mg	1510	210		1506	212	
Si	1667	556		1649	569	
O_B	−885	5		−824	5	
O_A	−1138	4		−1184	6	
O_I	−837	7		−849	7	
O_o	−890	6		−857	8	
H_I	112		81	132		77
H_o	154		77	104		79

by comparison of the results of Mulliken population analyses and PDOS calculated for both the 3D structure and a computational 2D layer. The computational layer contained all atoms of the 1:1 lizardite layer (layer group $P31m$), and the positions of individual atoms in both cases were identical. Naturally, input tolerances for evaluation of integrals were identical to those used in 3D calculations. The difference in energies per unit cell, $\Delta E = E_{total}$ (3D) − E_{total} (2D), was equal to 0.032 a.u., which represents ~0.0017% of E_{total} (3D). Such a small quantity is in good agreement with the assumption of weak forces holding adjacent 1:1 layers. However, because all calculations were made at the Hartree-Fock level, we cannot state that the calculated ΔE reflects the whole truth.

Figure 8 shows the changes in the O s band PDOS induced by layer-to-layer interactions: Mg and Si s and all p bands were not changed so dramatically. There are two striking features: First, although the main bands of O_A, O_o, and O_I are destabilized (i.e., moved toward higher energies) by the interactions with the adjacent layers, the O_B band is stabilized. Second, the O_o band is much more destabilized in comparison with the O_A and O_I bands. One possible interpretation of these changes is as follows. When an isolated 1:1 layer is approached by another layer, electron density is redistributed mainly because of the formation of hydrogen bonds. Clearly, the greatest effect would be on the atoms of first contact, i.e., O_B and OH_o. As a result, O_B atoms become more negative, and the difference in the charges within the OH group, $\Delta Q =$

TABLE 2. Selected interatomic distances (Å) and bond populations in the full structure (in $10^{-3}|e|$ units)

	Distance	Bond population
Si-O_B	1.646	+339
Si-O_A	1.616	+389
Mg-O_A	2.121	+48
Mg-O_I	2.082	+61
Mg-O_o	2.021	+72
⟨O-H⟩$_I$	0.794	+386
⟨O-H⟩$_o$	0.837	+391
H_o-O_B	2.220	+10
H_I-O_B	3.002	+5
O_B-O_A	2.682	−14
O_A-O_I	3.079	−3
O_A-O_o	2.676	−8
O_o-O_I	2.725	−8
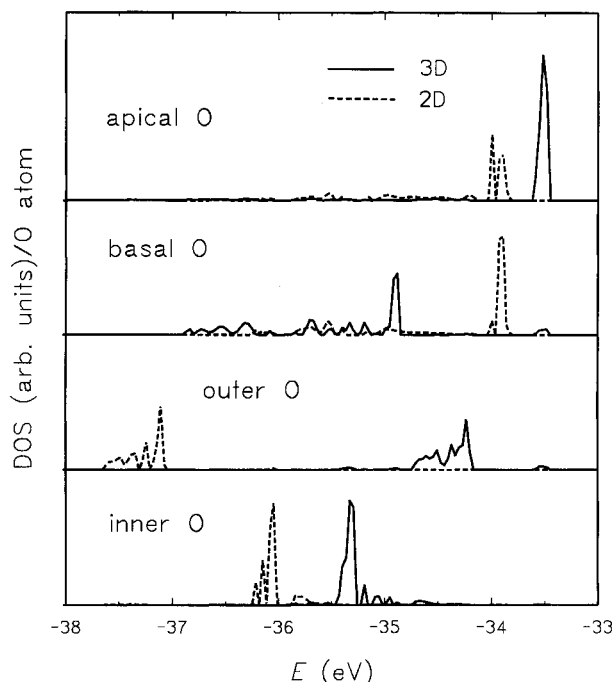
FIGURE 8. Comparison of PDOS calculated for a slab (2D) and the complete structure (3D).

$|Q(O_o)| - |Q(H_o)|$, increases (Table 1). Increased polarization of the O-H bond destabilizes the O_o contribution to the s band. Changes in the atomic charge in the inner OH group are then caused by a "chain reaction" initiated by a neighboring layer on OH_o, O_B, or both. However, because ΔQ is not in this case so large, corresponding shifts (Fig. 8) are smaller. It should be stressed again that this hypothesis assumes that hydrogen bonds are the main force holding 1:1 layers together and ignores the influence of long distance (dispersion) interactions.

REMARKS

This work has not touched on a very interesting feature recognizable in all accurately refined crystal structures of 1:1 phyllosilicates: All octahedral cations are shifted toward the outer OH groups, which causes the inner OH groups to be raised. (Such small shifts, though indisputable, often pass unnoticed, buried in so-called "average" interatomic distances.) This feature occurs in both lizardite 1T and lizardite 2H_1, dickite (Joswig and Drits 1986), nacrite (Zheng and Bailey 1994), and cronstedtite (Smrčok et al. 1994). This phenomenon and the bonding conditions in Al- and Fe-bearing 1:1 phyllosilicates warrant further study.

ACKNOWLEDGMENTS

References Cited

Benco, Ľ., and Smrčok, Ľ. (1994) Ab initio calculated electron densities for tetrahedral sheet [$H_2Si_2O_5$] in phyllosilicates. Physics and Chemistry of Minerals, 21, 401–406.

Causà, M., Dovesi, R., Pisani, C., and Roetti, C. (1986) Electronic structure and stability of different crystal phases of magnesium oxide. Physical Review B, 33, 1308-1316.

D'Arco, P., Causà, M., Roetti, C., and Silvi, B. (1993) Periodic Hartree-Fock study of weakly bonded layer structure: Brucite $Mg(OH)_2$. Physical Review B, 47, 3522–3529.

Dovesi, R., Causà, M., Orlando, R., Roetti, C., and Saunders, R.V. (1990) Ab initio approach to molecular crystals: A periodic Hartree-Fock study of crystalline urea. Journal of Chemical Physics, 92(12), 7402–7411.

Dovesi, R., Pisani, C., Roetti, C., Causà, M., and Saunders, V.R. (1992) CRYSTAL92: An ab initio electron LCAO-Hartree-Fock program for periodic systems. QCPE Program no. 577. Quantum Chemistry Program Exchange. Indiana University, Bloomington, Indiana.

Hess, A.C., and Saunders, V.R. (1992) Periodic ab initio Hartree-Fock calculations of the low-symmetry mineral kaolinite. Journal of Physical Chemistry, 96, 4367–4374.

Huzinaga, S. (1965) Gaussian-type functions for polyatomic systems I. Journal of Chemical Physics, 42, 1293–1302.

Joswig, W., and Drits, V.A. (1986) The orientation of the hydroxyl groups in dickite by X-ray diffraction. Neues Jahrbuch für Mineralogie Monatshefte, H.1, 19–22.

Mellini, M. (1982) The crystal structure of lizardite 1*T*: Hydrogen bonds and polytypism. American Mineralogist, 67, 587–598.

Mellini, M., and Zanazzi, P.F. (1987) Crystal structures of lizardite-1*T* and lizardite-2*H*₁ from Coli, Italy. American Mineralogist, 72, 943–948.

Nada, R., Catlow, C.R.A., Dovesi, R., and Saunders, V.R. (1992) An ab initio Hartree Fock study of the ilmenite-structured $MgSiO_3$. Proceedings of Royal Society London A, 436, 499–509.

Pissani, C., Dovesi, R., and Roetti, C. (1988) Hartree-Fock ab initio treatment of crystalline systems: Lecture Notes in Chemistry, volume 48. Springer, Berlin.

Sherman, D.M. (1991) Hartree-Fock band structure, equation of state, and pressure-induced hydrogen bonding in brucite, $Mg(OH)_2$. American Mineralogist, 76, 1769–1772.

Smrčok, Ľ., Ďurovič, S., Petříček, V., and Weiss, Z. (1994) Refinement of the crystal structure of cronstedtite 3*T*. Clays and Clay Minerals, 42, 544–551.

Zheng, H., and Bailey, S.W. (1994) Refinement of the nacrite structure. Clays and Clay Minerals, 42, 46–52.